MERIT Internship report (domestic company)

Shotaro Baba
PhD student, Sagawa group
Department of Applied Physics
MERIT 8th

1 Outline of Internship

- Place: KYOCERA Corporation, Minatomirai Research Center Research institute for advanced materials and devices, Department of fundamental technology research, Electromagnetic field technology section
- Period: 11/1/2021–11/30/2021
- Research Topic: The tradeoff between the power and the efficiency of quantum many-body engines when crossing a quantum phase transition

2 Outline of Workshop

I researched my topic remotely. In addition, we visited the office three times and viewed the facilities of Kyocera Minatomirai Research Center. The main content of the internship was the experimental study of large-size quantum many-body systems using D-Wave's quantum annealing machine. Specifically, we studied the trade-off between the driving speed and the efficiency of work extraction from a heat engine on a quantum many-body system.

3 Research Summary

Since the numerical cost of quantum many-body systems increases exponentially with the size of the system, experimental verification is important for the analysis of large system sizes and high-dimensional systems. In this study, we used a quantum annealing machine with hundreds to thousands of qubits to study large quantum many-body systems that are difficult to analyze numerically.

D-Wave's quantum annealing machine is a superconducting quantum qubit system developed for optimization problems and is available as a cloud service. The latest machine consists of more than 5,000 qubits operating at about 15.4mK, allowing the user to design how the qubits are coupled together. Therefore, it is

possible to perform various physics experiments at low temperatures in large quantum many-body systems. Previous studies of physics experiments using this quantum annealing machine include the phase transition in the three-dimensional Ising model [1], the KT transition in the two-dimensional transverse field Ising model [2], the competition between thermal and quantum fluctuations (spin ice) [3], many-body localization [4], topological defects [5], a thermal machine that accelerates the transfer of heat from a high-temperature heat bath to a low-temperature heat bath by external work [6].

In this work, we realize a quantum heat engine that extracts work from thermodynamic cycles on a quantum annealing machine and observe the trade-off between efficiency and driving speed via a quantum phase transition. Theoretical studies of heat engines with quantum phase transitions include, for example, the proposal of an example of achieving Carnot efficiency with finite power [7, 8] and the study of scaling described by the critical exponent between driving speed and work [9, 10]. Another example of an experimental superconducting quantum cubit system is the implementation of a heat engine and verifies the fluctuation theorem in a small system on IBM Q [11].

Near the quantum phase transition point, the energy difference between the ground state and the first excited state becomes exponentially small in the system size in the case of a first-order phase transition. Therefore, in adiabatic quantum computation, if we want to change the magnetic field, etc. while the quantum state remains in the ground state, we need to change it slowly as the energy difference becomes smaller in order to avoid excitation (time $T \sim \Delta^{-2}$,where Δ is a energy difference). The work taken out in the isothermal process is the difference in free energy F. Therefore, if excitations occur, the free energy of a final state will increase and the work extracted will be small. In order to extract a large amount of work in the isothermal process, it is necessary to reduce the excitation energy, and to do so, it is necessary to move slowly. This is the cause of the trade-off between the driving speed and the efficiency through the quantum phase transition, which is the focus of this study. The scaling between the density of defects (kinks) due to excitation from the ground state ρ_{kink} and the drive time t_a has already been observed in annealing machines [5], with the following relationship.

$$\rho_{\text{kink}} \propto t_a^{-\frac{d\nu}{1+z\nu}}. \tag{1}$$

Here, ν is the critical exponent for a correlation length, d is the dimension of the system, and z is dynamical critical exponents. In the one-dimensional transverse-field Ising model, $\nu = z = d = 1$ and $d\nu/(1 + z\nu) = 1/2$.

This section describes the specific setup for this study. The target system of

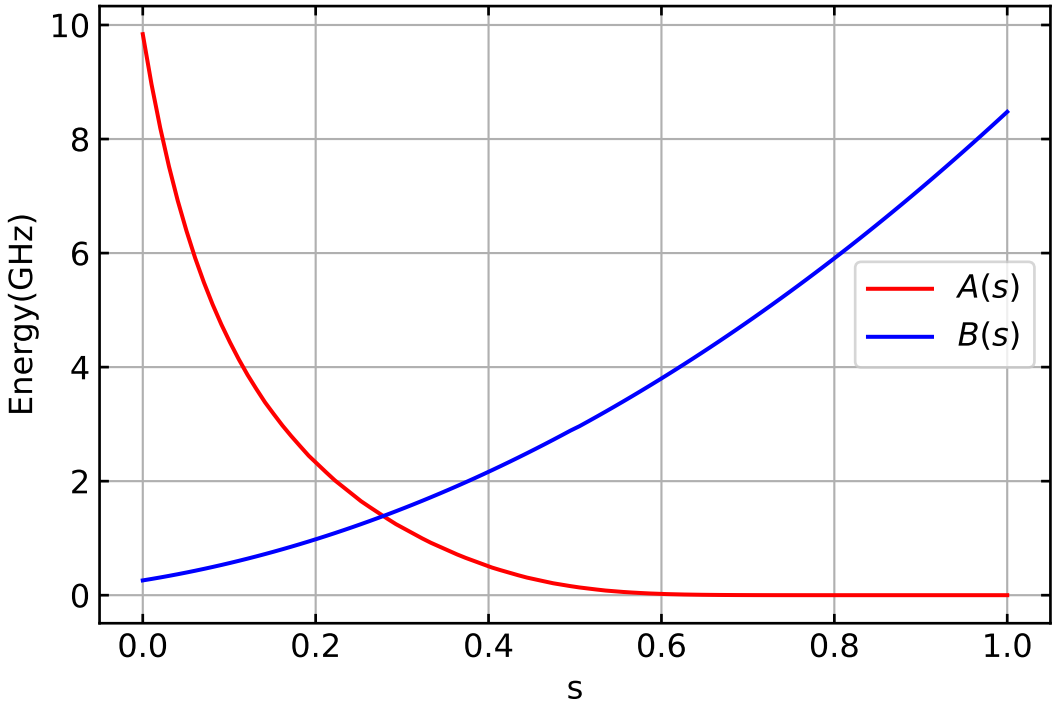

Figure 1: The vertical axis represents $A(s)$, $B(s)$. The horizontal axis represents s

our investigation is the one-dimensional transverse-field Ising model (TFIM)

$$H = -\frac{A(s)}{2}\sum_{i=1}^{L}\sigma_i^x - \frac{B(s)}{2}\sum_{i=1}^{L}\sigma_i^z\sigma_{i+1}^z,$$

where the number of qubits $L = 2000$, s is the parameter which controls the value of functions $A(s)$, $B(s)$. $A(s)$, $B(s)$ are shown in Figure 1. These functions are determined by D-Wave and cannot be changed by the user. The phase transition point is $s \sim 0.28$, below which the ground state is in the disordered phase, and above which it is in the ferromagnetic phase. The constructed cycle is illustrated in Figure 2. This cycle can be thought of as an analogy of the Stirling cycle (the original Stirling cycle is an isothermal operation A in contact with a high-temperature heat bath). First, the control parameter s is set to 1, and the initial state (I) is randomly sampled from product states. This corresponds to the thermal equilibrium state at infinite temperature. Next, (A) the control parameter s is quenched from 1 to a certain value $\bar{s}$. It can be shown analytically that the work done here is zero. (Since the trace of the Hamiltonian before and after the

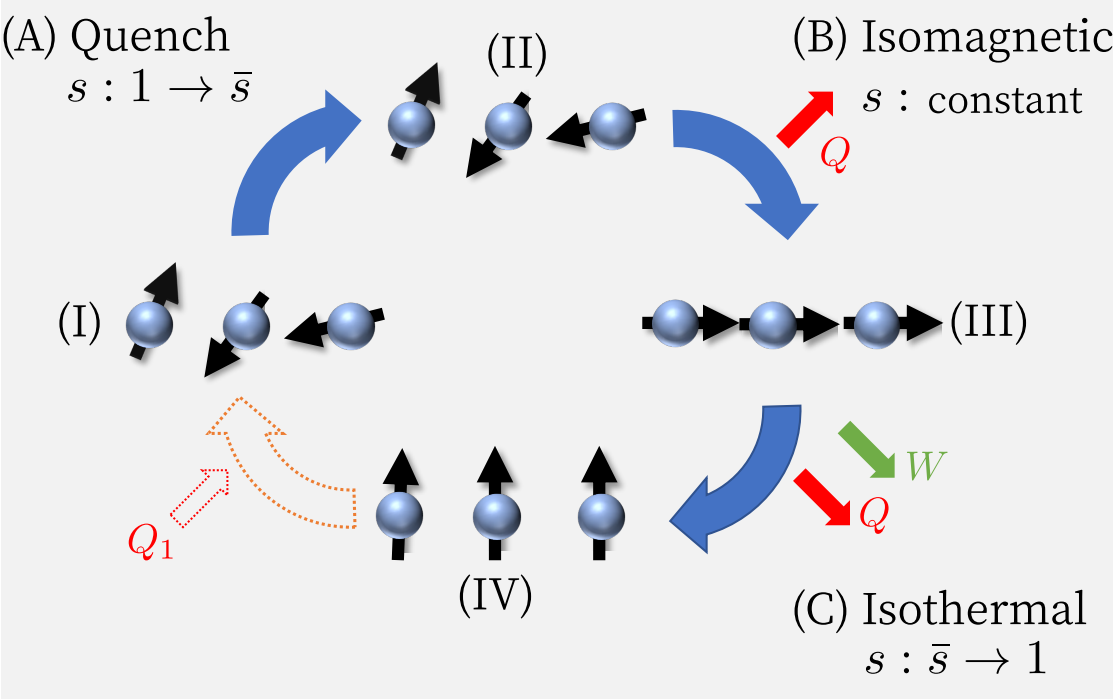

Figure 2: The cycle constructed in this study. The system is assumed to be always in contact with a low-temperature heat bath.

transition is zero and hence the energy of the random state is zero, the energy difference before and after the quench is zero assuming that the state remains random.) In the experiment, the actual time is not zero but $(1-\bar{s})/2\mu s^{-1}$ because the change of control parameters is limited to a finite speed $v = 2\mu s$. Next, we perform constant-field cooling at (B)$s = \bar{s}$. In other words, the system thermalizes in contact with a low-temperature heat bath (the low-temperature environment in the annealing machine). In this experiment, the constant field cooling was performed for 350μs. Finally, (C) the control parameter s is driven from $\bar{s}$ to 1 at a constant rate. The energy $E_{\rm IV}$ of the final state is now measured. From here, the cycle is completed by a virtual thermalization at infinite temperature. By repeating this cycle many times while sampling a random state as the initial state, the distribution of energy in the final state $P(E_{\rm IV})$ is obtained. An example of the time dependence of the control parameter is shown in Figure 3. In this cycle, only stroke C has a work input or output. By varying the rate of isothermal manipulation of this stroke C, we measure the energy $E_{\rm IV}$ of the final state. The ideal maximum work is the difference in free energy between (III) and (IV)

$$W_{\rm max} = F(T_C, \bar{s}) - F(T_C, 1), \tag{2}$$

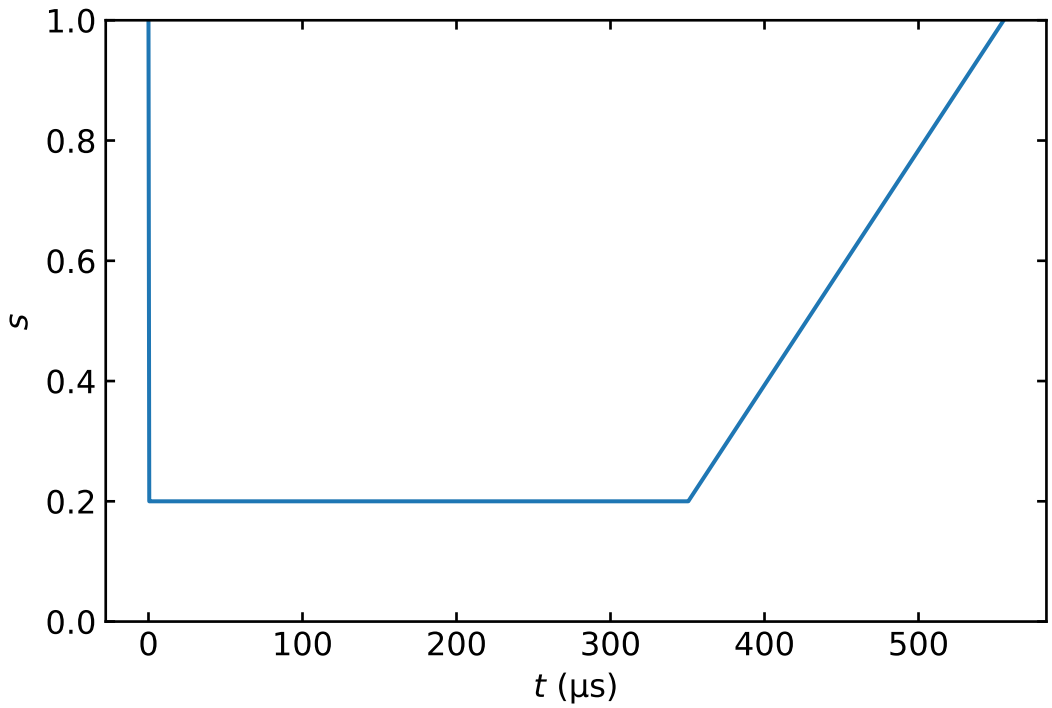

Figure 3: An example of the time dependence of the control parameter$s$ where $\bar{s} = 0.2$ and driving speed is $v = 2^{-8}\mu s^{-1}$.

and the corresponding maximum efficiency is

$$\eta_{\max} = W_{\max}/Q_1, \tag{3}$$

where Q_1 is the difference in internal energy between (III) and (IV), and is the heat absorbed during this cycle. The actual work done in this cycle is estimated as the difference between the maximum work $W_{\max}$ and the excitation energy ε_{ex}

$$W = W_{\max} - \varepsilon_{\text{ex}}. \tag{4}$$

The corresponding efficiency is

$$\eta = W/Q_1. \tag{5}$$

The excitation energy is calculated as the expectation value of the distribution of the difference between the analytical energy $E(T_C, s = 1)$ at temperature T_C and the measured final state energy E_{IV}

$$\varepsilon_{\text{ex}} = \mathbb{E}\left[P(E_{IV}) - E(T_C, s = 1)\right]. \tag{6}$$

The expectation value is taken with respect to the set of initial states.

In preparation for the work estimation, we will estimate the effective temperature of the quantum annealing machine. It is known that the effective temperature of a quantum annealing machine $T_{\rm eff}$ differs from the physical temperature (15.4mK) due to a lot of noise and errors. Therefore, we estimate the effective temperature needed to calculate the analytical free energy and other parameters. Specifically, we perform a maximum likelihood estimate of the effective temperature which determine the Boltzmann distribution that explains the energy distribution $P(E_{\rm IV})$ of the final state (IV), which is the thermal equilibrium state obtained by slowing down the stroke C. More precisely, the method is called pseudo-likelihood estimate and we maximize the following quantities

$$\Gamma(\beta) = -\frac{1}{LD}\sum_{d=1}^{D}\sum_{l=1}^{L}\ln\left[1+\exp\left(-2\beta\sigma_l^d\sum_{m\in\delta_l}\sigma_m^d\right)\right], \tag{7}$$

where D is the number of samples, $\sigma_l^d \pm 1$ is the spin of site l in the dth sample (The Hamiltonian is a classical Ising model in the final state $s = 1$, and this classical spin configuration is measurable), and δ_l is the set of the indexes of the neighboring sites of site l. The initial states were randomly sampled 1000 times, and 10 trials were performed for each. Therefore, the sample size is 10000 samples for each control parameter $\bar{s}$ and drive speed v. Figure 4 shows the results of estimating the inverse temperature $\beta = 1/k_{\rm B}T$ while changing the drive speed v for isothermal operation of stroke C. The slower we drive the stroke C, the more it converges to $\beta = 2.5$. In other words, the thermal equilibrium states obtained when moving slowly corresponds to $\beta = 2.5$. When moved quickly, the excitation results in a distribution that cannot be explained by the Gibbs distribution, and the estimation is failed. This inverse temperature $\beta = 2.5$ corresponds to 162.734mK, which is in the range estimated by previous study [13]. In the following calculations, the inverse temperature corresponding to the cold heat bath is assumed to be $\beta_C = 2.5$.

Next, we give the analytical results for the ideal cycle. The one-dimentional quantum TFIM is solvable by the Jordan-Wigner transformation and allows us to calculate the internal energy, the free energy F, and the internal energy of the Gibbs distribution for a given inverse temperature β [14]. Using these analytical quantities, the ideal maximum work $W_{\rm max}$ and maximum efficiency $\eta_{\rm max}$ can be calculated. The free energy density is shown in Figure 5. The ideal maximum work output is shown in Figure 6. The ideal maximum efficiency is shown in Figure 7. These results shows that the work output and the efficiency are maximum near the phase transition point $s \sim 0.28$ for the ideal cycle.

Next, we describe the experimental results on the annealing machine. First, we observe the scaling of the excitation energy corresponding to the driving speed of the control parameters during the isothermal process C. According to the Kibble-

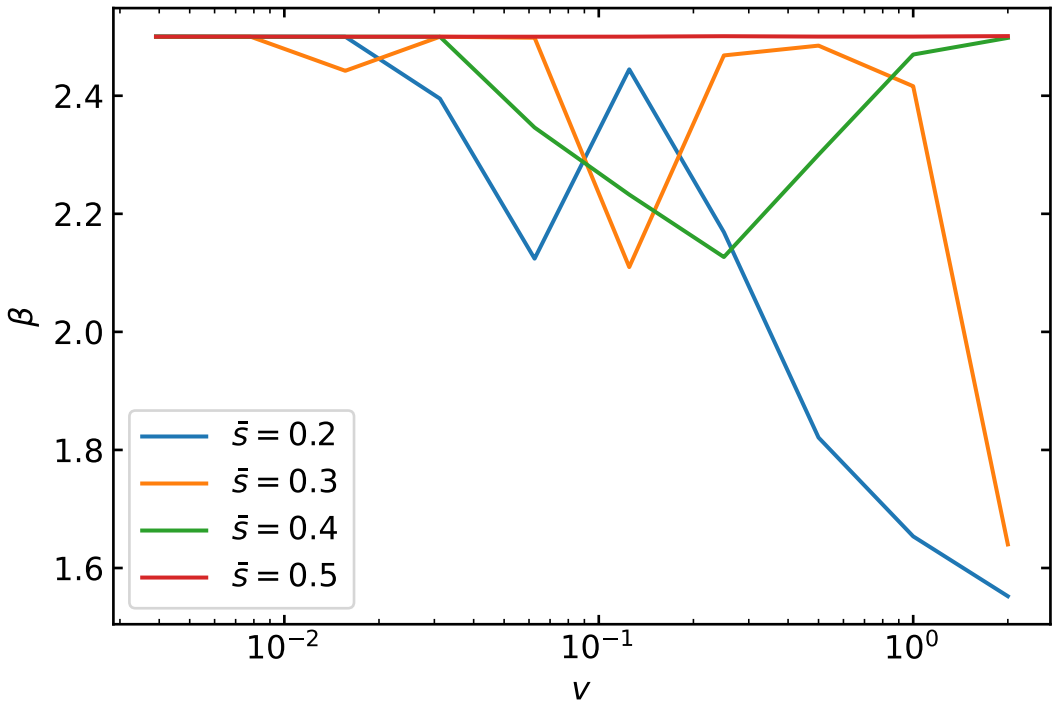

Figure 4: Results of maximum likelihood estimation of driving speed v and inverse temperature β for isothermal operation of stroke C. It can be seen that the slower the stroke is moved, the more it converges to $\beta = 2.5$. The energy is nondimensionalized so that the ground energy of the Hamiltonian at $s = 1$ is -1. The inverse temperature is also a dimensionless quantity.

Zurek mechanism [15], the density of kinks or defects increases exponentially with the driving speed when passing through the transition point at finite speed. Therefore, a similar scaling is expected to be observed for the excitation energy. In the above cycle, we measured and calculated the $\varepsilon_{\mathrm{ex}}$ for each $\bar{s}$ while varying the driving speed v of the isothermal operation of the stroke C. The results are shown in Figure 8. The measurement data is the same as that used for the estimation of the effective temperature described above, and the sample size is 10000 samples for each control parameter $\bar{s}$ and drive speed v, respectively. The Kibble-Zurek mechanism describes scaling through a transition point at finite speed, and the power-law scaling is observed in Figure 8 for $\bar{s} = 0.2,\ 0.3$ through the vicinity of the transition point. A least-squares fit to the result for this $\bar{s} = 0.2,\ 0.3$, assuming the functional form $\varepsilon_{\mathrm{ex}} = av^b$, yielded a power $b = 0.41(1)$. Figure 9 shows a plot of the functional form av^b with the parameters obtained by this least-squares

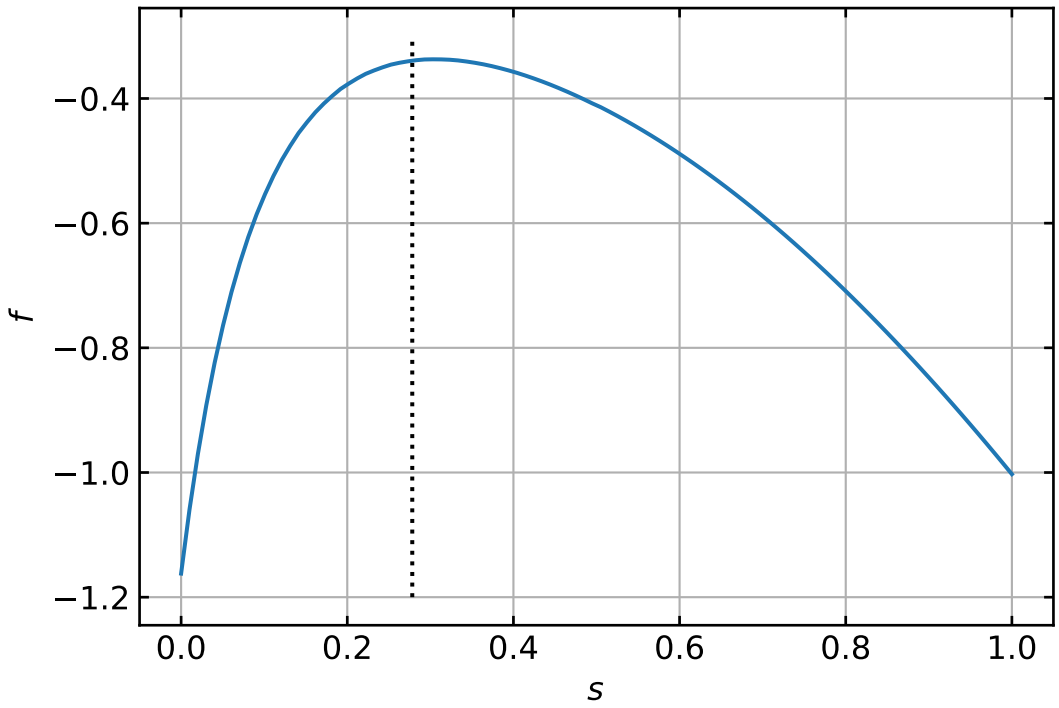

Figure 5: The free energy density of 1D quantum TFIM in the thermodynamic limit at $\beta = 2.5$. The inverse temperature corresponding to cold bath is$\beta = 2.5$. The vertical dotted line represents phase transition point $s \sim 0.28$.

fit, together with the measurement results. The error bars represent the standard deviation of the measurement results. The prediction of the Kibble-Zurek mechanism for the isolated 1D quantum TFIM is $b = \frac{d\nu}{1+z\nu} = 0.5$. On the other hand, this power tends to be smaller for open systems [5]. Therefore, it is a reasonable result.

Finally, from $\varepsilon_{\mathrm{ex}}$, we calculate the relationship between the driving speed and the work Eq. (4), efficiency Eq. (5). The results for the work are shown in Figure 10, and the results for the efficiency are shown in Figure 11. In the region where the driving speed is small, it can be seen that the largest amount of work and efficiency can be obtained at $\bar{s} = 0.3$, which passes through near the phase transition point. This is because the free energy of the Gibbs distribution corresponding to the temperature of the cold heat bath becomes the largest near the transition point (Figure 5). This is mainly due to the fact that the ground state energy becomes large near the transition point where the gap becomes small. This cause the difference in the energy between state (III) and state (IV) large. The

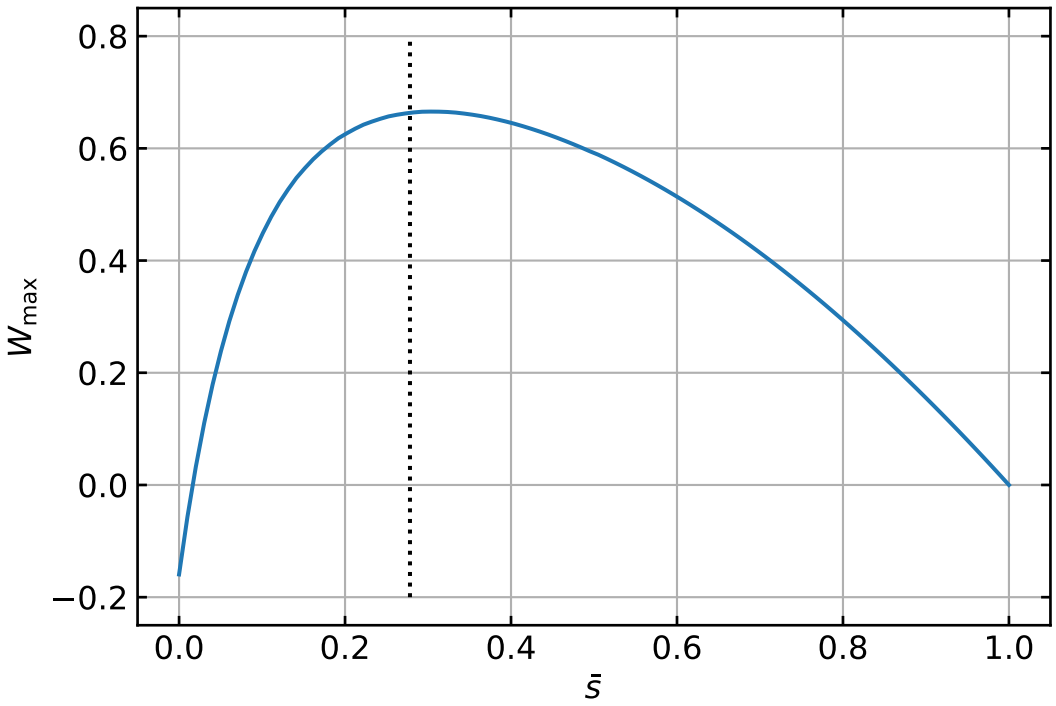

Figure 6: The maximum work output in the ideal cycle. The inverse temperature corresponding to cold bath is $\beta = 2.5$. The energy is nondimensionalized so that the ground energy of the Hamiltonian at $s = 1$ is -1. The vertical dotted line represents phase transition point $s \sim 0.28$.

large difference in the energy between the state results in large work. On the other hand, in the case of $\bar{s} = 0.2,\ 0.3$, the work and efficiency become significantly lower when the driving speed is increased compared to the case at a $\bar{s}$ far from the phase transition point. Even when going through near the phase transition point, in the case of $\bar{s} = 0.3$, the efficiency is larger than that of $\bar{s} = 0.4$ up to a driving speed larger than the speed where the work of $\bar{s} = 0.3$ gets smaller than that of $\bar{s} = 0.4$. This is because the heat input Q_1 in the next virtual stroke gets smaller due to the excitation energy in stroke C. These results indicate that in order to increase the amount of the work and the efficiency, it is necessary to apply a transverse magnetic field until near the phase transition point ($\bar{s} \sim 0.28$). However, this has the disadvantage of greatly reducing the efficiency when the drive speed is increased. This relationship of decreasing efficiency with increasing drive speed indicates the trade-off between power and efficiency in an engine passing near the transition point.

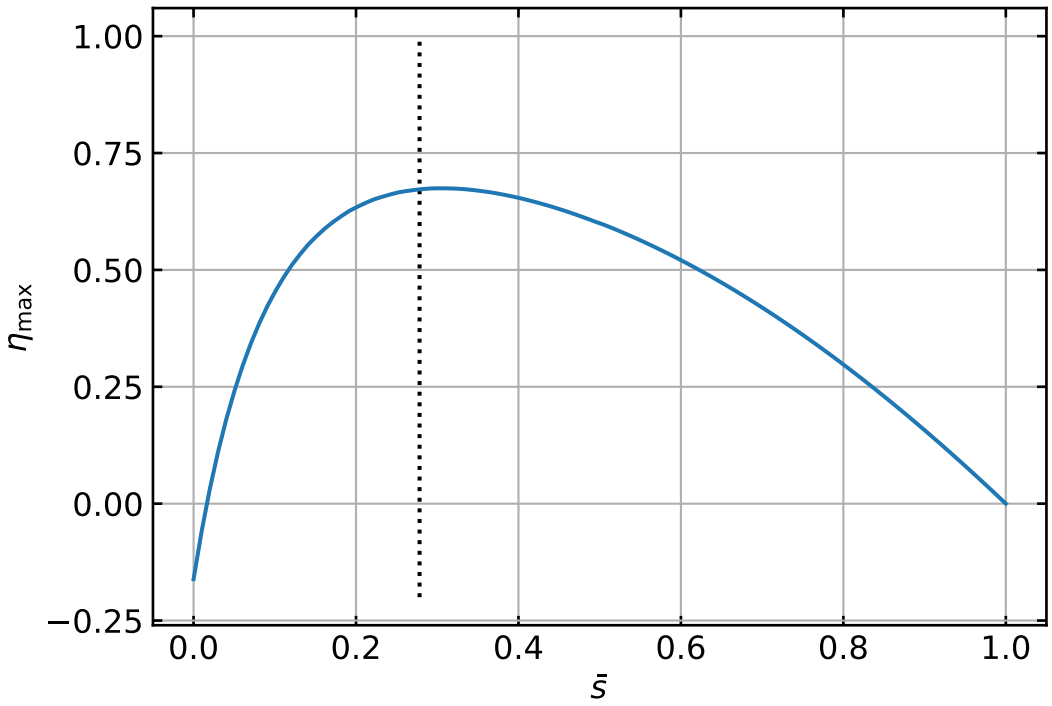

Figure 7: The maximum efficiency in the ideal cycle. The inverse temperature corresponding to cold bath is $\beta = 2.5$. The vertical dotted line represents phase transition point $s \sim 0.28$.

In this work, we experimentally study the trade-off between the efficiency of work extraction and the driving speed in a thermodynamic cycle realized on the quantum transverse field Ising model with system size $L = 2000$. A power scaling between the driving speed and the excitation energy through the quantum phase transition point is observed, which can be explained by the Kibble-Zurek mechanism. Due to this power scaling, a trade-off between power and efficiency is observed. As far as I know, there is no experimental study on the trade-off between power and efficiency in a large quantum many-body system of system size $L = 2000$, and this is a novel result.

As a future development, we may use the thermodynamic uncertainty relation [16,17] derived from the detailed fluctuation theorem to estimate the work. In this study, due to experimental limitations, we actually measured the distribution of the final state energy $P(E_{\mathrm{IV}})$. Therefore, we did not measure the work directly, but estimated it by subtracting the excitation energy from the ideal maximum work. This estimate is based on the analytical free energy density and the analytical

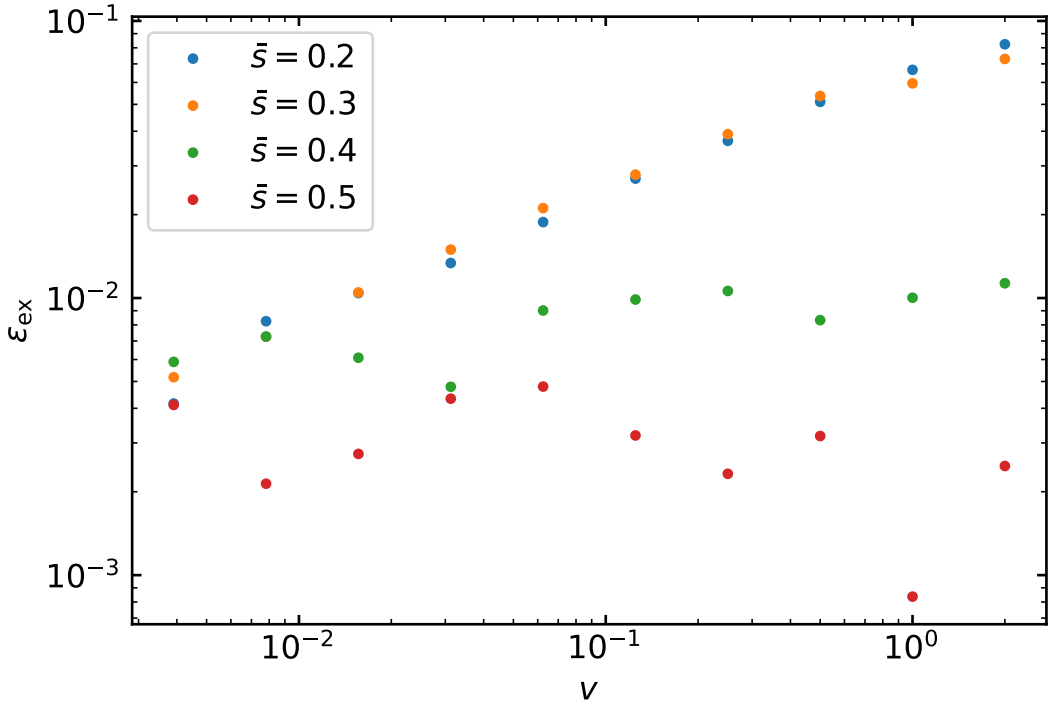

Figure 8: The result of measurements and calculations for $\varepsilon_{\mathrm{ex}}$ while changing the rate v of the isothermal process C for each control parameter $\bar{s}$ where we perform isomagnetic cooling. We observe the power-law scaling for $\bar{s} = 0.2,\ 0.3$, where passing through near the phase transition. The energy is nondimensionalized so that the ground energy of the Hamiltonian at $s = 1$ is -1.

internal energy density in the thermodynamic limit. Because of the existence of finite size effects in the case of system size $L = 2000$, the finite size effect needs to be taken into account. In addition, since the estimated temperature is also used, the temperature estimation error is also included. Furthermore, the excitation energy is estimated based on the assumption that the heat transfer in and out of the isothermal process of stroke C can be explained by an isothermal quasi-static process. This is because the energy scale of the Hamiltonian is ∼GHz, while the control parameters are driven on a ∼µs scale, and the heat input and output will not deviate significantly from the isothermal quasi-static process. In other words, if more heat is flowing out than in the isothermal quasistatic process, the actual excitation energy will be larger than the estimated amount (the extra heat flowing out means that the excitation is actually larger). In addition, since the quench of stroke A has a finite velocity, there may be a input or output of work. Therefore,

it is important to estimate the work directly without making any assumptions, and it is worthwhile to use thermodynamic uncertainty relations to estimate the work.

4 Acknowledgement

I would like to deeply thank Dr. Mashiko and the staff of Electromagnetic field technology section for their continued advice and support during this internship. I would also like to express my gratitude to the people in the Minatomirai Research Center for guiding me during the tour in the Center. Finally, I would like to express my sincere gratitude to my supervisor, Prof. Sagawa, my MERIT advisor, Prof. Ogata, and MERIT program for giving me this chance.

References

[1] R. Harris, Y. Sato, A. J. Berkley, M. Reis, F. Altomare, M. H. Amin, K. Boothby, P. Bunyk, C. Deng, C. Enderud, S. Huang, E. Hoskinson, M. W. Johnson, E. Ladizinsky, N. Ladizinsky, T. Lanting, R. Li, T. Medina, R. Molavi, R. Neufeld, T. Oh, I. Pavlov, I. Perminov, G. Poulin-Lamarre, C. Rich, A. Smirnov, L. Swenson, N. Tsai, M. Volkmann, J. Whittaker, and J. Yao, *Phase transitions in a programmable quantum spin glass simulator*, Science **361**, 6398 (2018) .

[2] A. D. King, J. Carrasquilla, J. Raymond, I. Ozfidan, E. Andriyash, A. Berkley, M. Reis, T. Lanting, R. Harris, F. Altomare, K. Boothby, P. I. Bunyk, C. Enderud, A. Fréchette, E. Hoskinson, N. Ladizinsky, T. Oh, G. Poulin-Lamarre, C. Rich, Y. Sato, A. Y. Smirnov, L. J. Swenson, M. H. Volkmann, J. Whittaker, J. Yao, E. Ladizinsky, M. W. Johnson, J. Hilton, and M. H. Amin, *Observation of topological phenomena in a programmable lattice of 1,800 qubits*, Nature **560**, 7719 (2018) .

[3] A. D. King, C. Nisoli, E. D. Dahl, G. Poulin-Lamarre, and A. Lopez-Bezanilla, *Qubit spin ice*, Science **373**, 6554 (2021) .

[4] J. L. C. d. C. Filho, Z. G. Izquierdo, A. Saguia, T. Albash, I. Hen, and M. S. Sarandy, *Observation of many-body localization in an experimental quantum annealer*, `arXiv:2108.06762`.

[5] Y. Bando, Y. Susa, H. Oshiyama, N. Shibata, M. Ohzeki, F. J. Gómez-Ruiz, D. A. Lidar, S. Suzuki, A. del Campo, and H. Nishimori, *Probing the*

universality of topological defect formation in a quantum annealer: Kibble-Zurek mechanism and beyond, Phys. Rev. Res. **2**, 3 (2020) .

[6] L. Buffoni and M. Campisi, *Thermodynamics of a Quantum Annealer*, Quantum Sci. Technol. **5**, 3 (2020) .

[7] M. Campisi and R. Fazio, *The power of a critical heat engine*, Nat. Commun. **7**, 11895 (2016) .

[8] Y. H. Ma, S. H. Su, and C. P. Sun, *Quantum thermodynamic cycle with quantum phase transition*, Phys. Rev. E **96**, 2 (2017) .

[9] Z. Fei, N. Freitas, V. Cavina, H. T. Quan, and M. Esposito, *Work Statistics across a Quantum Phase Transition*, Phys. Rev. Lett. **124**, 17 (2020) .

[10] R. B. S, V. Mukherjee, U. Divakaran, and A. Del Campo, *Universal finite-time thermodynamics of many-body quantum machines from Kibble-Zurek scaling*, Phys. Rev. Res. **2**, 4 (2020) .

[11] A. Solfanelli, A. Santini, and M. Campisi, *Experimental Verification of Fluctuation Relations with a Quantum Computer*, PRX Quantum **2**, 3 (2021) .

[12] E. Aurell and M. Ekeberg, *Inverse ising inference using all the data*, Phys. Rev. Lett. **108**, 9 (2012) .

[13] M. Benedetti, J. Realpe-Gómez, R. Biswas, and A. Perdomo-Ortiz, *Estimation of effective temperatures in quantum annealers for sampling applications: A case study with possible applications in deep learning*, Phys. Rev. A **94**, 2 (2016) .

[14] P. Pfeuty, *The one-dimensional Ising model with a transverse field*, Ann. Phys. **57**, 1 (1970) .

[15] T. W. Kibble, *Topology of cosmic domains and strings*, J. Phys. A **9**, 8 (1976) .

[16] A. M. Timpanaro, G. Guarnieri, J. Goold, and G. T. Landi, *Thermodynamic Uncertainty Relations from Exchange Fluctuation Theorems*, Phys. Rev. Lett. **123**, 9 (2019) .

[17] Y. Zhang, *Comment on "Fluctuation Theorem Uncertainty Relation" and "Thermodynamic Uncertainty Relations from Exchange Fluctuation Theorems"*, `arXiv:1910.12862`.

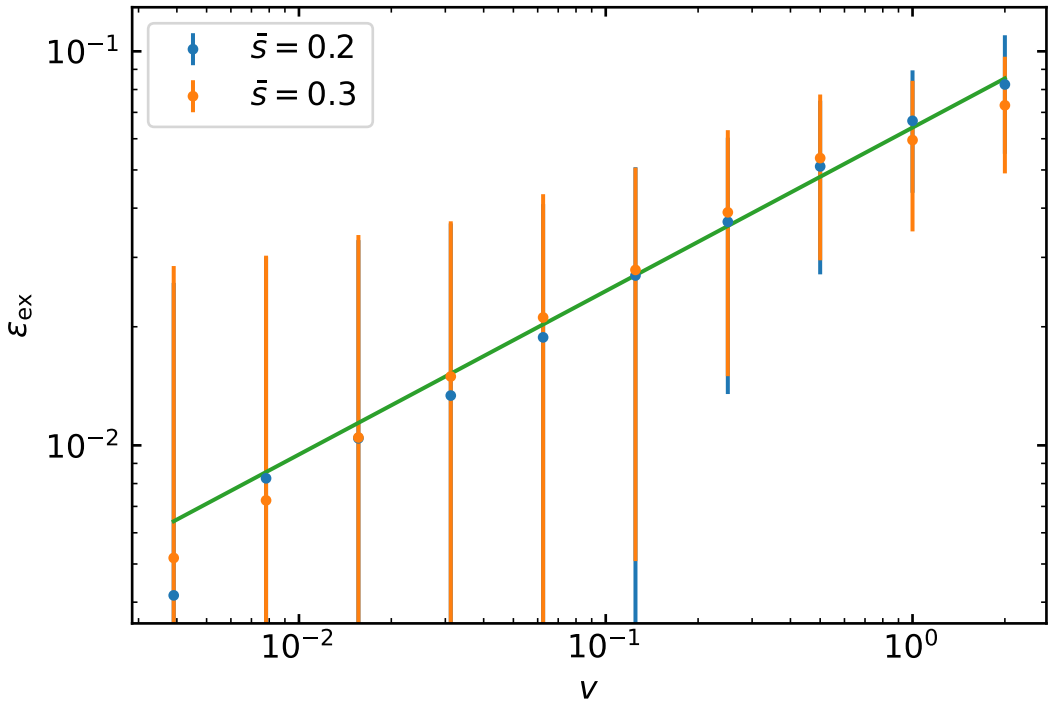

Figure 9: A function obtained by least-squares fitting of the excitation energy results for the $\bar{s} = 0.2,\ 0.3$ is plotted together with the measurement results. The least-squares fit was performed assuming a functional form that shows power-like scaling $\varepsilon_{\mathrm{ex}} = av^b$. The error bars represent the standard deviation of the measurement results. In the region where v is small, the error bars are large due to the larger accumulative noise received while driving the control parameters. The energy is nondimensionalized so that the ground energy of the Hamiltonian at $s = 1$ is -1.

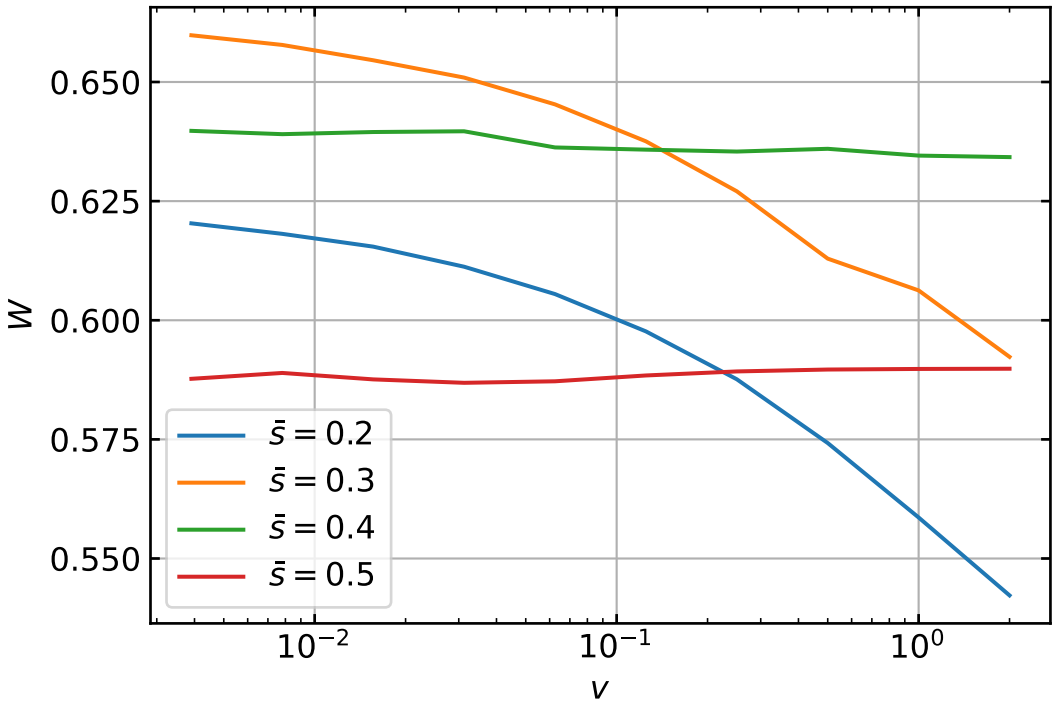

Figure 10: The driving speed through the stroke C is plotted on the horizontal axis and the vertical axis is the work for each control parameter $\bar{s}$ where we perform isomagnetic cooling. In the region where the drive speed v is small, $\bar{s} = 0.3$, which performs isomagnetic cooling near the transition point, outputs the most work. On the other hand, in the case of $\bar{s} = 0.2,\ 0.3$, which passes through near the transition point, the output work decreases significantly when the drive speed is increased. The energy is nondimensionalized so that the ground energy of the Hamiltonian at $s = 1$ is -1.

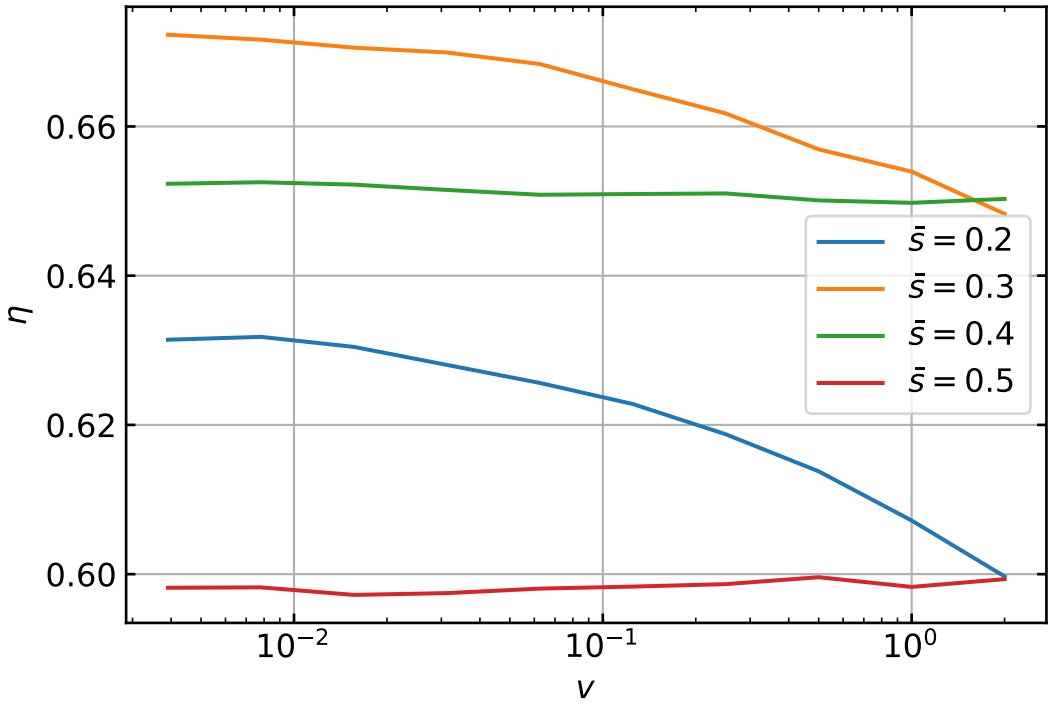

Figure 11: The driving speed through the stroke C is plotted on the horizontal axis and the vertical axis is the efficiency for each control parameter $\bar{s}$ where we perform isomagnetic cooling. In the region where the drive speed v is small, the highest efficiency is obtained when the isomagnetic cooling is performed near the transition point $\bar{s} = 0.3$. On the other hand, the efficiency of $\bar{s} = 0.2,\ 0.3$, which passes through near the transition point, decreases significantly when the drive speed is increased.